JOURNAL OF THE BALKAN GEOPHYSICAL SOCIETY, Vol. 6, No. 1, February 2003, p. 21 – 36, 8 figs.

Seismic modeling of marine reflection data from Ionian Sea

E. Kokinou* and A. Vafidis*

*Applied Geophysics Lab., Dep. Of Mineral Resources, Eng. Technical Univ. of Crete, Chania, GREECE 73100.
E-mails: ekokinou@mred.tuc.gr; vafidis@mred.tuc.gr

Abstract: *Seismic modeling was performed in order to interpret the data from a seismic reflection survey conducted across the western margin of the Hellenic arc in Ionian sea. The synthetic seismograms were calculated utilizing the Finite difference method. The migrated seismic section along the surveyed seismic line showed complex geologic structures such as a diapiric flower structure near Kefallinia island. Velocity analysis was performed on the field data in order to obtain velocity models for the Kefallinia diapir and the sedimentary basin east of Kefallinia diapir. For the sedimentary basin, the root mean square (RMS) velocities of selected events for the real and synthetic data are in very good agreement. Major reflection events have been identified and are attributed to the top of Plio-Quaternary, Upper Miocene-Lower Pliocene and Middle-Miocene sediments. The synthetic seismograms for three shot gathers proved useful in recognizing the seismic events on the real data for the diapiric structure. The reflection from the top of the diapiric intrusion is present on both real and synthetic seismograms. The diapir, consisting of Triassic evaporites, intercepts the Plio-Quaternary and Upper Miocene-Lower Pliocene sedimentary layers.*

INTRODUCTION

In the last decades, several techniques have been developed for simulating propagation of seismic wavefields in the earth. Recent advances in computing based on the subdivision of the computational sequence into parallel components make more tractable realistic simulations. In forward modeling the wavefield is generated by using ray tracing or solving wave equations. In order to gain an acceptable geological model, comparisons are often made between the synthetic and observed seismograms.

Á basic problem in theoretical seismology is to determine the wave response of a given model tï the excitation of an impulsive source by solving the wave equations. The acoustic wave equation may be solved to evaluate the waveform by considering only compressional waves (P-waves). Á more complete approach is to study the vector displacement field using the full elastic wave equation. More realistic simulations can be performed through the heterogeneous elastic wave equation. These methods allow the modeling of seismic wave propagation in complex laterally and vertically varying structures, containing combinations of isotropic and anisotropic layers. In order to calculate the elastic response of a model, second order differential equations must be solved simultaneously. Instead of solving this second order system, equivalent first order systems are solved numerically for isotropic media (Vafidis, 1988) and for transversely isotropic media (Tsingas et al., 1990). These systems consist of the basic equations of motion and the stress-strain relations.

In seismic wave-equation modeling discrete-coordinate methods are applied such as the finite difference methods (Kelly et al., 1976; Vafidis et al, 1992), the finite element methods (Smith, 1975; Marfurt, 1984) and other methods that combine time advancing algorithms and integral transformations with respect to space variables such as the Fourier transform method (Reshef et al., 1988) and the pseudo-spectral method (Kosloff and Baysal, 1982; Mikhailenko and Korneev, 1984).

Wave properties such as attenuation and dispersion require a more sophisticated set of equations, such as Biot's equations for porous media. Biot (1956a,b) developed a theory from the view point of continuum mechanics for wave motion in a porous elastic solid saturated with a viscous compressible fluid. In Biot's theory attenuation of wave energy is due to the motion of the pore fluid relative to the rock frame. de Ia Cruz and Spanos (1985) constructed macroscopic wave equations for elastic porous media filled with viscous fluid by using volume averaging techniques in conjunction with physical arguments. Wave dispersion and dissipation in these models are mainly due to the viscous fluid motion relative to the solid matrix.

Numerical solution of Biot's acoustic wave equations is given by Hassanzadeh (1991) and a second order finite difference solution to Biot's poroelastic wave equations is proposed by Zhu and McMechan (1991). Dai et al. (1995) reformulated Biot's and de Ia Cruz-Spanos equations into first order differential system which enables one to obtain the fluid and solid particle velocities and stress components and also the fluid pressure. For the two-dimensional problem of wave propagation in porous media, SÇ waves decouple from Ñ and SV waves. The Biot's model predicts the existence of one shear and two compressional waves with a faster and a slower velocity. However, mathematical models based on this type of mechanism suffer many times from excessive free parameters that makes realistic wave simulations for exploration targets very difficult or impossible.

Considerable progress has been also made in seismic wave attenuation for a single phase material. In this context, seismic attenuation is taken to describe any irreversible energy losses, other than those due to spherical divergence, reflections, transmissions and mode conversions, which a seismic wave experiences as it propagates through a medium. Emmerich and Korn (1987) used a generalized Maxwell body to approximate an arbitrary Q law yielding a second order differential equation system with extra intermediate variables for SH waves. Á first order hyperbolic system has been derived for 2-D anelastic acoustic wave motion by Vafidis et al. (1993) based on the generalized Maxwell body approximation and solved with an explicit finite difference scheme. Furthermore, Blanch et al. (1993) used finite difference schemes to model wave propagation in 2-D and 3-D viscoelastic media. Ïn the other hand, Carcione et al. (1988a,b) used pseudo-spectral methods for simulation of viscoacoustic wave propagation.

The synthetic seismograms generated by the Finite difference method are useful because:

1) the method takes into account both the vertical and lateral velocity variations,
2) the synthetic seismograms help in identifying seismic events related to complex geological structures,
3) simpler models are used for a given level of fit to the data and
4) the synthetic seismograms can assess the final model in terms of errors, resolution and non – uniqueness (Zelt, 1999).

The comparison of real and synthetic seismograms has been used in many cases in order to study and explain the geological conditions of the research area (Brokesova et al., 2000; Brew et al., 1998; Frenje et al., 1998). The similarity of the seismograms generated through modeling compared with the real data has been proven striking very often (Larkin et al., 1996; Hollinger, 1997).

This paper presents the finite difference seismic modeling method as it is applied on seismic data from the Ionian sea. A short description of the seismic experiment is followed by the presentation of the processing of the seismic data. Then, the finite difference method is described. The geologic setting for the area under investigation is also presented. The results of the seismic simulations for Kefallinia diapir and sedimentary basin models are discussed in detail.

THE ION-7 SEISMIC LINE

A Deep Seismic Profiling (DSP) experiment was carried out in 1992 with the support of the European Union (JOULE STREAMERS PROJECT), in order to obtain information about the structure of the crust, and probably the upper mantle (Hirn et al., 1996). Seven seismic lines of total length 700 Km were scanned in the central Mediterranean sea. One of these lines namely ION – 7 crosses the Ionian basin (Fig. 1).

The seismic data were recorded by Geco-Prakla's M/V Bin Hai 511 which towed a 36 – airgun tuned array with a capacity of 7118 inch^3 (about 120 l) (McBride et al., 1994). A 180 channel streamer array produced a 30-fold normal incidence reflection profile. The shot interval was 75 m, the receiver interval 25 m, the minimum offset 180 m, and the sampling interval 8 ms. The seismic data (Fig. 2) has been reprocessed using the PROMAX 2D package.

Table 1 shows the processing steps. Wave equation multiple rejection (WEMR) and deconvolution methods were applied on the shot records. The RMS – stacking velocities were picked from the velocity spectrum by comparing the uncorrected and the NMO – corrected data. Thereinafter the RMS velocities were converted to interval ones using Dix equation. F-K filtering and surface consistent deconvolution have been also applied to reduce the coherent noise and the lateral reflections. Poststack Kirchoff migration removed distortions due to lateral velocity variations and improved lateral resolution. On a selected portion of the stacked section, depth migration was additionally applied to image diapirism. The instantaneous attributes computed by Hilbert transform were used in the interpretation of the stacked and migrated section.

THE FINITE DIFFERENCE METHOD

Finite difference methods have been used successfully to solve numerically the seismic wave equation. Explicit schemes are more popular in two-or three-dimensional problems since their solution is straightforward. The spatial interval is chosen so that the model fits into the computer memory. On the other hand the spatial interval should be kept small so that grid dispersion effects are minimal. Once the spatial interval has been chosen, the stability condition specifies the maximum time step allowed to avoid instabilities. Stability also depends on the model's maximum velocity. Finite difference methods are computationally expensive and the efficiency of the method greatly depends on the technique of calculating the response.

For seismic propagation, a finite difference algorithm is utilized which is second order accurate in time and fourth order in space (PROMAX 2D Reference). Its formulation does not require numerical differentiation of the medium parameters. It describes acoustic wave propagation in a two dimensional heterogeneous medium. In order to calculate the earth's response the equivalent first-order hyperbolic system of equations given below is solved numerically. This system consists of the basic equations of motion in the x and z directions, namely:

$$\rho\,(x,z)\frac{\partial}{\partial t}\dot{u}\,(x,z,t) = \frac{\partial}{\partial x}p(x,z,t) \qquad (1)$$

$$\rho\,(x,z)\frac{\partial}{\partial t}\dot{w}\,(x,z,t) = \frac{\partial}{\partial z}p(x,z,t) \qquad (2)$$

and the pressure-strain relation after taking the first time derivatives:

$$\frac{\partial}{\partial t}p(x,z,t) = K(x,z)\left[\frac{\partial}{\partial z}\dot{w}(x,z,t) + \frac{\partial}{\partial x}\dot{u}\,(x,z,t)\right] \qquad (3)$$

where the dot denotes time derivative, $\dot{u}$(x,z,t) and $\dot{w}$ (x,z,t) represent the vertical and horizontal components of the particle velocity, respectively, p(x,z,t) denotes the pressure field, ρ(x,z) is the density of the medium and K(x,z) is the bulk modulus. Equations (1)-(3) can be written in matrix form as

$$\frac{\partial}{\partial t}\begin{bmatrix} p \\ \dot{u} \\ \dot{w} \end{bmatrix} = \begin{bmatrix} 0 & K & 0 \\ 1/\rho & 0 & 0 \\ 0 & 0 & 0 \end{bmatrix} \frac{\partial}{\partial x}\begin{bmatrix} p \\ \dot{u} \\ \dot{w} \end{bmatrix} + \begin{bmatrix} 0 & 0 & K \\ 0 & 0 & 0 \\ 1/\rho & 0 & 0 \end{bmatrix} \frac{\partial}{\partial z}\begin{bmatrix} p \\ \dot{u} \\ \dot{w} \end{bmatrix}$$

or (4)

$$\frac{\partial}{\partial t}U = A\frac{\partial}{\partial x}U + B\frac{\partial}{\partial z}U$$

which is a first-order hyperbolic system.

Dispersion analysis indicates that the shortest wavelength in the model needs to be sampled at six grid points/wavelength. The source is implemented by specifying the initial conditions applied to both particle velocity and pressure and using the source insertion principle of Alterman and Karal (1968). A buried line source is chosen with a Gaussian time excitation function.

ÔHE KEFALLINIA DIAPIR AND THE SEDIMENTARY BASIN EAST OF THE DIAPIR

The seismic profile ION-7 of total length 180 km crosses the western margin of the Hellenic arc (HA) from the deep Ionian basin (southwest) to the Gulf of Patras (northeast). It is located at the western part of the External Hellenides which formed during Tertiary times as a result of the convergence between the Eurasia continent and Apulia microplate. In the area under investigation there are easterly dipping thrust faults, elongated anticlines, diapiric movements and “decollement” surfaces (Kamberis, 1996; Hirn et al., 1996). The western part of the line ION – 7 is located in the Ionian abyssal plain (IoAP) and its eastern part corresponds to the Hellenic Arc (HA) (Fig. 2).

Geological, seismological, magnetic, gravity, geothermal and GPS studies in Ionian Sea contributed in the interpretation of the migrated seismic section (Kokinou, 2002). The migrated section (Figs. 3 and 4) shows the Kefallinia diapir as well as the sedimentary basin east of the diapir. Kefallinia diapir involves a positive flower structure of Triassic evaporites (Fig. 3). The signal to noise ratio in the center of the anticline is very small. The upper layer corresponds to Plio – Quaternary (P – Q) sediments intercepted by the diapirism and followed by the Upper Miocene – Lower Pliocene (Mis – Pli) sediments. The Mesozoic Carbonates of Ionian (IO) and Paxos (Px) zones are present to the east of the diapir. In this region, the faulting due the intrusion of the Triassic evaporites influences all the layers (Kokinou, 2002).

For the sedimentary basin (Fig. 4) the top layer represents the Plio – Quartenary (P- Q) sediments. The layer from 0.5 s TWT to 1.2 s TWT corresponds to the Upper Miocene – Lower Pliocene (Mi – Pli) sediments, followed by the Middle – Miocene (Mid?) sediments. The deeper layers are attributed to the Mesozoic (Me) sequence and Triassic evaporites (Ev) (Kokinou, 2002). The Mesozoic sequence and the Triassic evaporites are interrupted by faults. All layers are almost parallel and slightly dipping.

SEISMIC WAVE PROPAGATION SIMULATIONS

The finite difference method divides the subsurface into a very fine two-dimensional grid. Within each rectangular grid point, velocity and density values are constant and seismic waves can accurately propagate through the grid. The main disadvantage of this method is that the computation time depends on the characteristic frequency of the waveform. Run times increase approximately as the cube of frequency and as the ratio of maximum velocity to minimum velocity in the model.

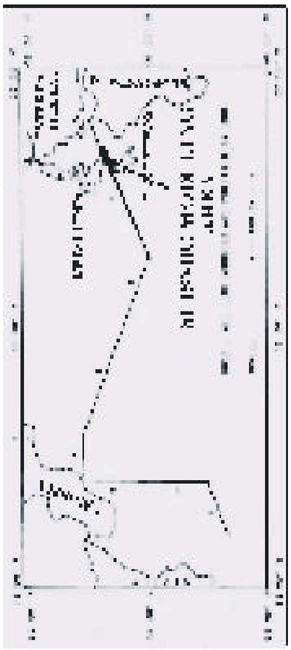

FIG 1. Map of STREAMERS—lines and seismic modeling area.

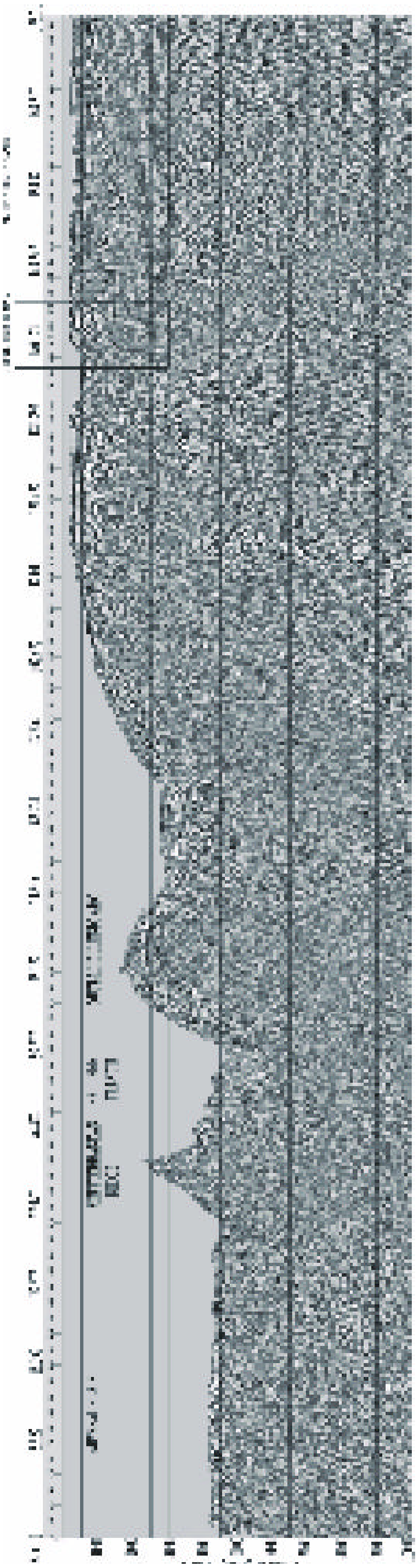

FIG 2. Stacked section for seismic line ION7 (vertical exaggeration = 3:2).

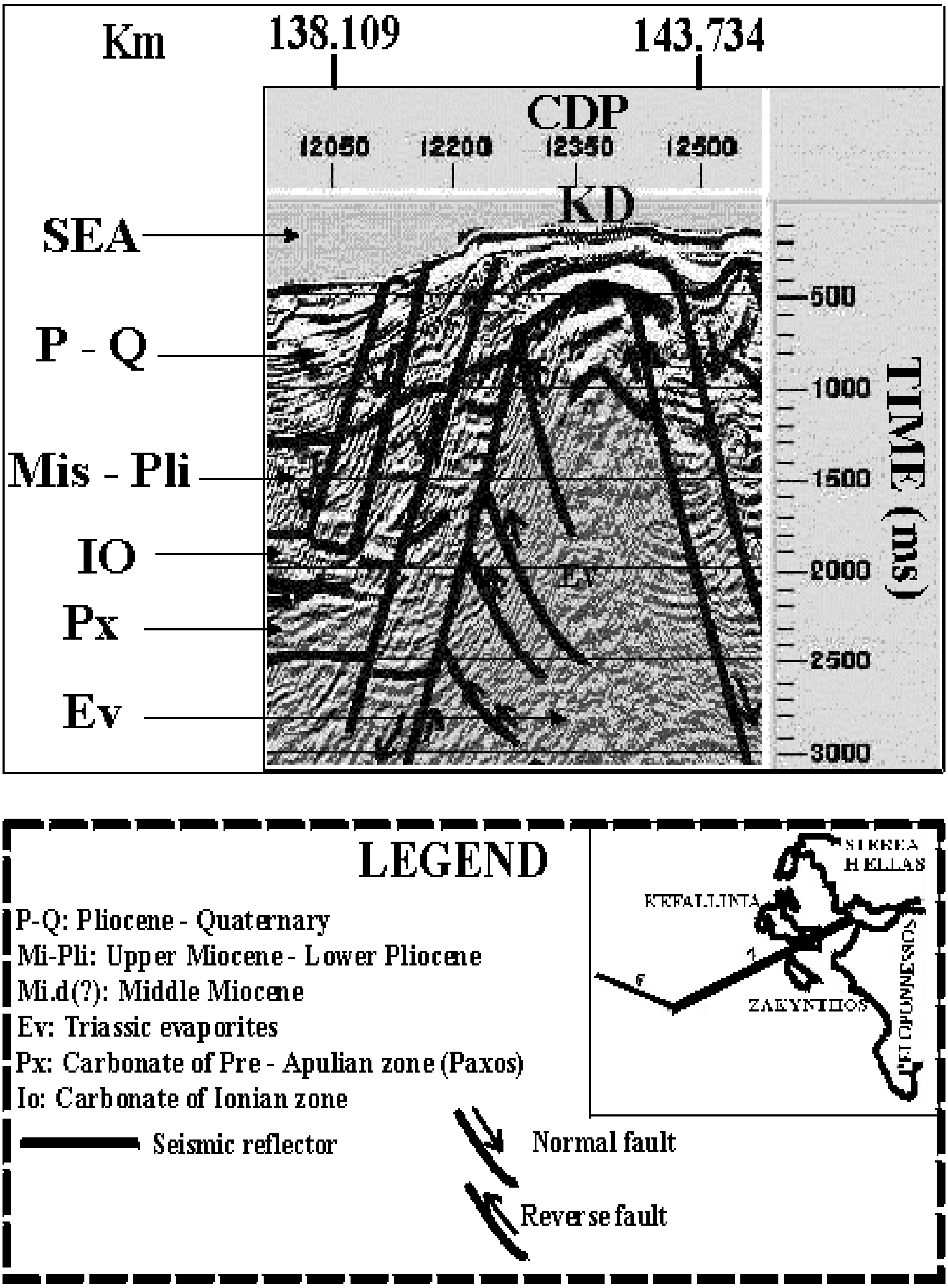

FIG. 3. Migrated and interpreted section of the Kefallinia Diapir.

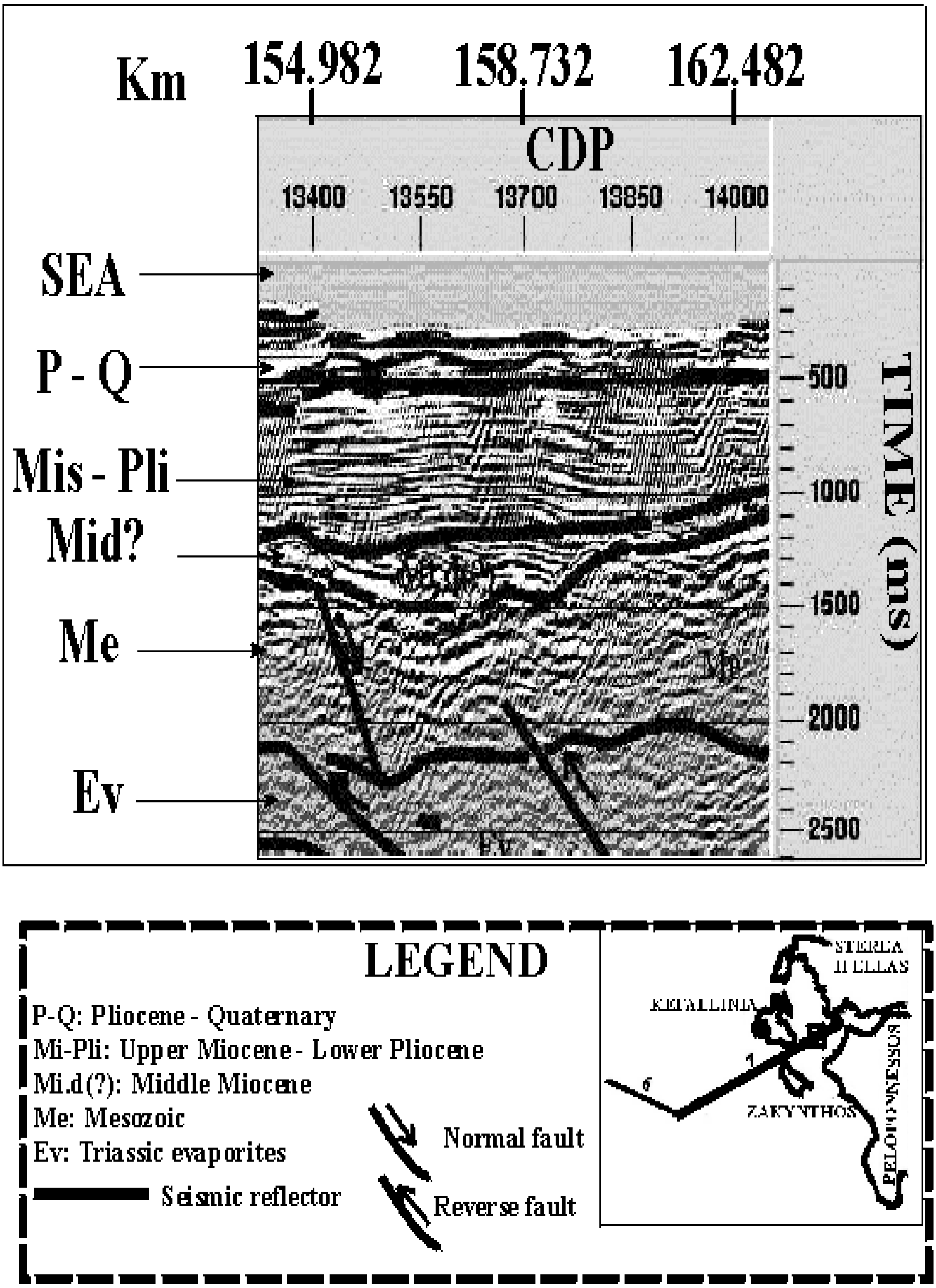

FIG. 4. Migrated and interpreted section of the sedimentary basin.

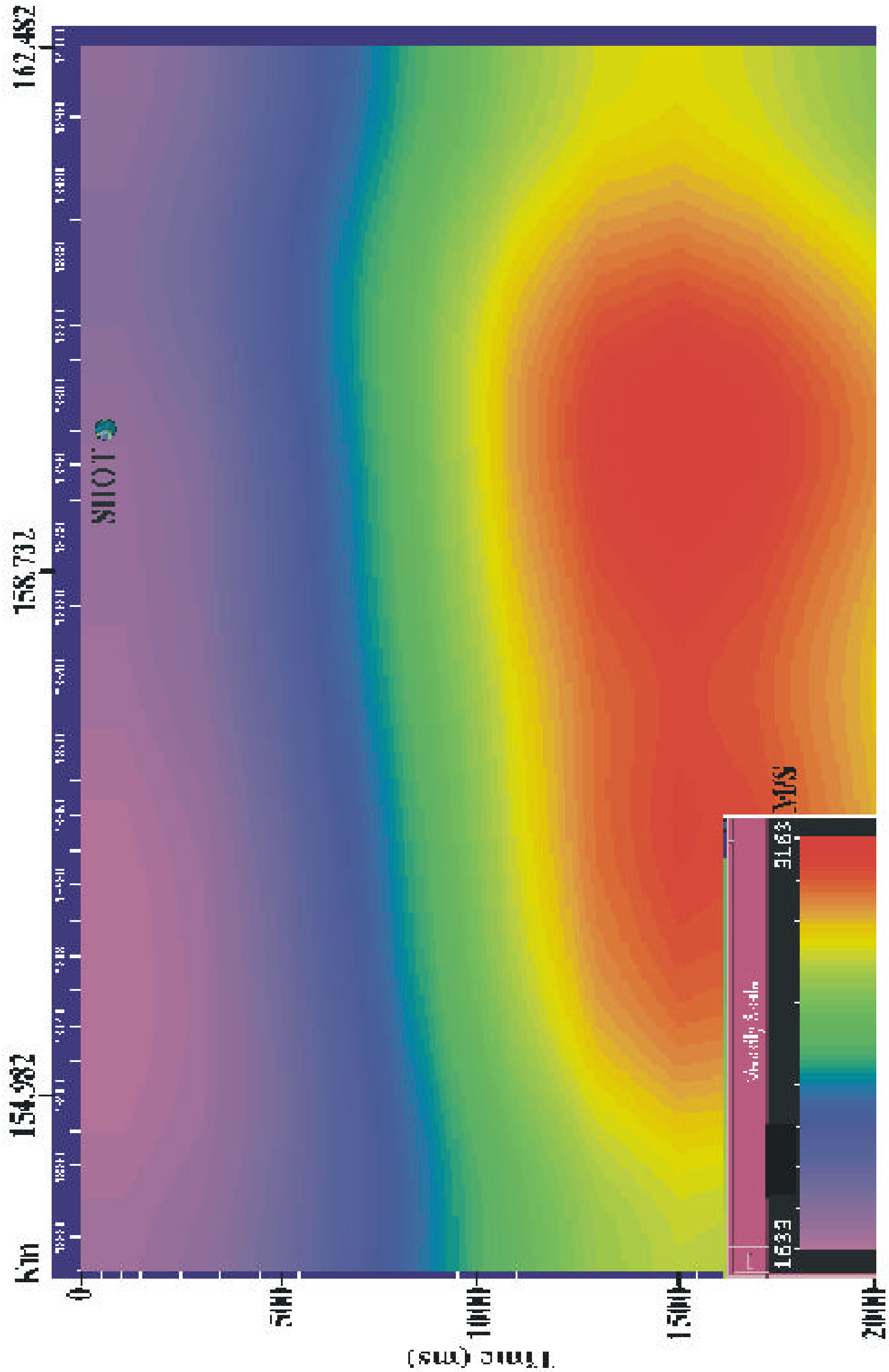

FIG. 5a. Interval velocities of the sedimentary basin model

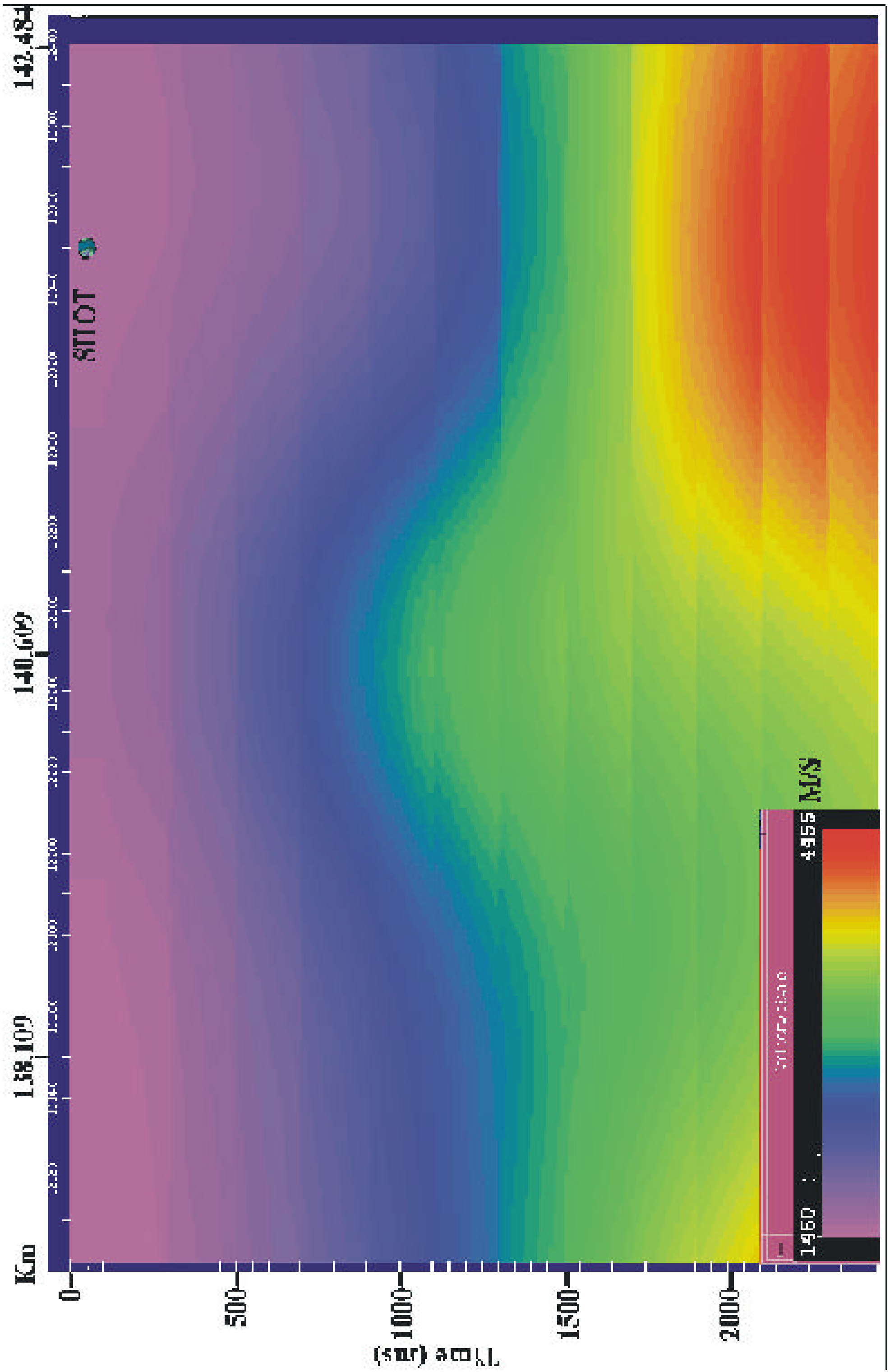

FIG. 5b. Interval velocities of the Kefallinia Diapir

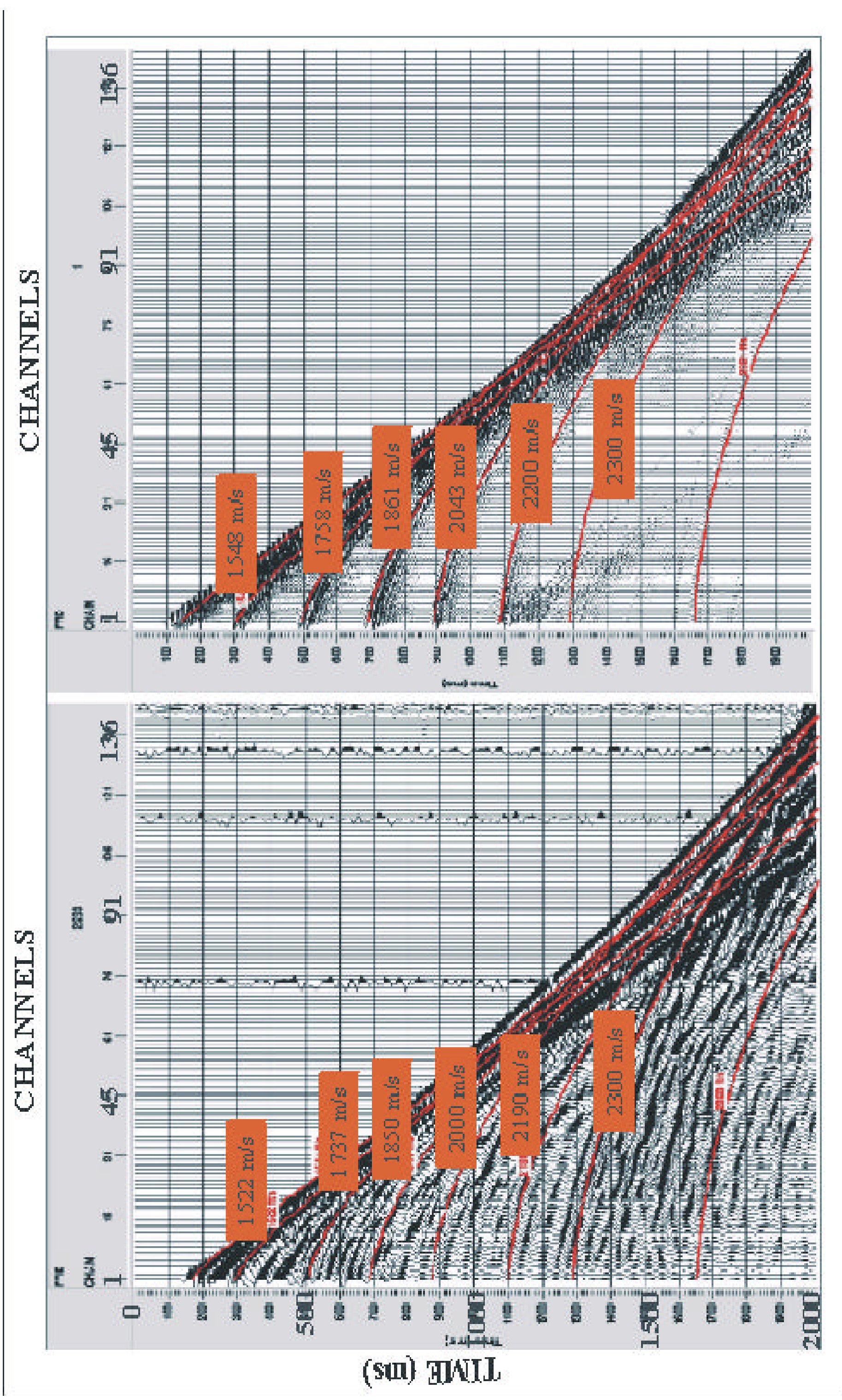

FIG. 6 Sedimentary basin model. Common shot gather (a) field and (b) synthetic data.

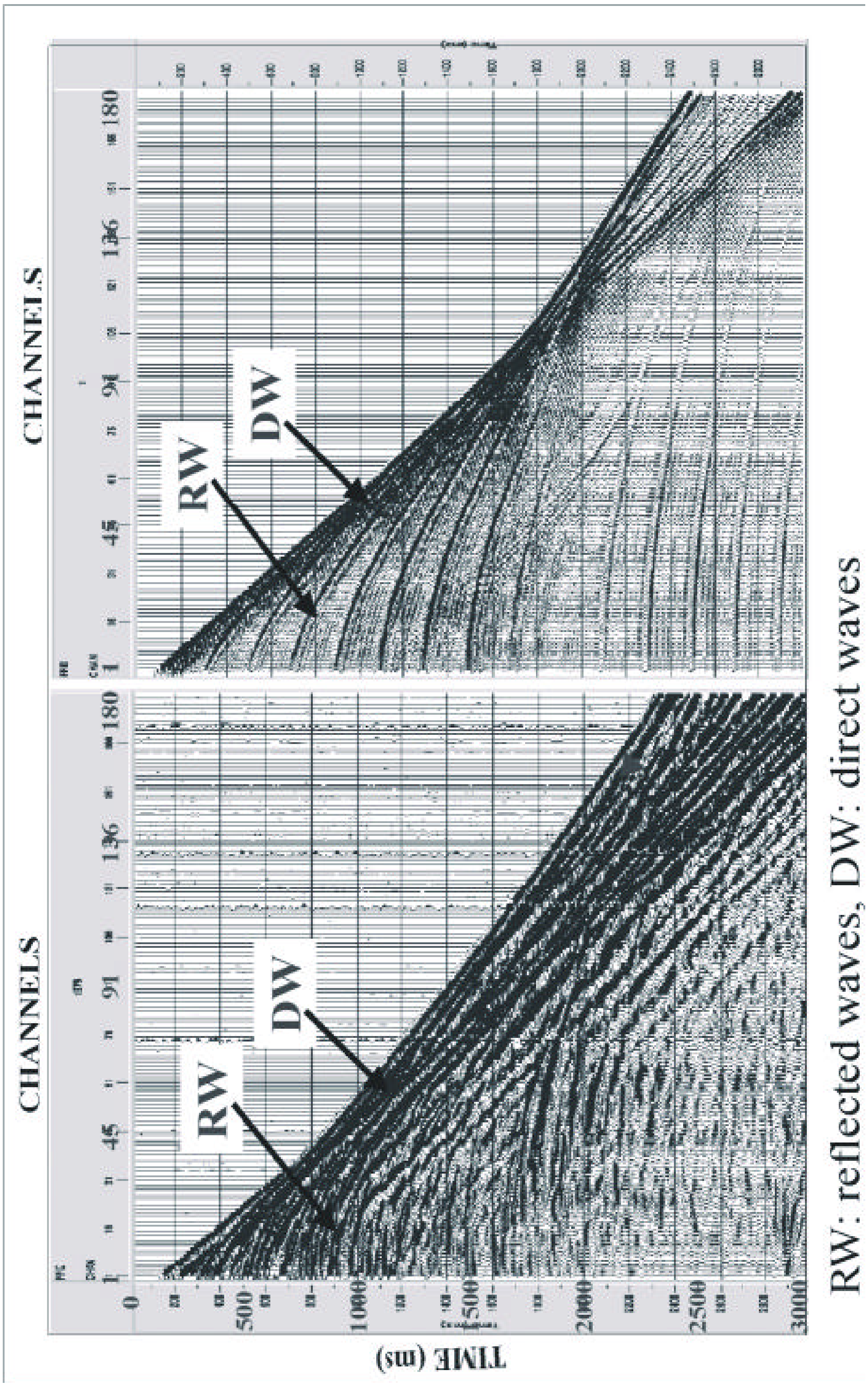

(a) (b)

FIG. 7. Kefallinia diapir model. Common shot gather (a) field and (b) synthetic data.

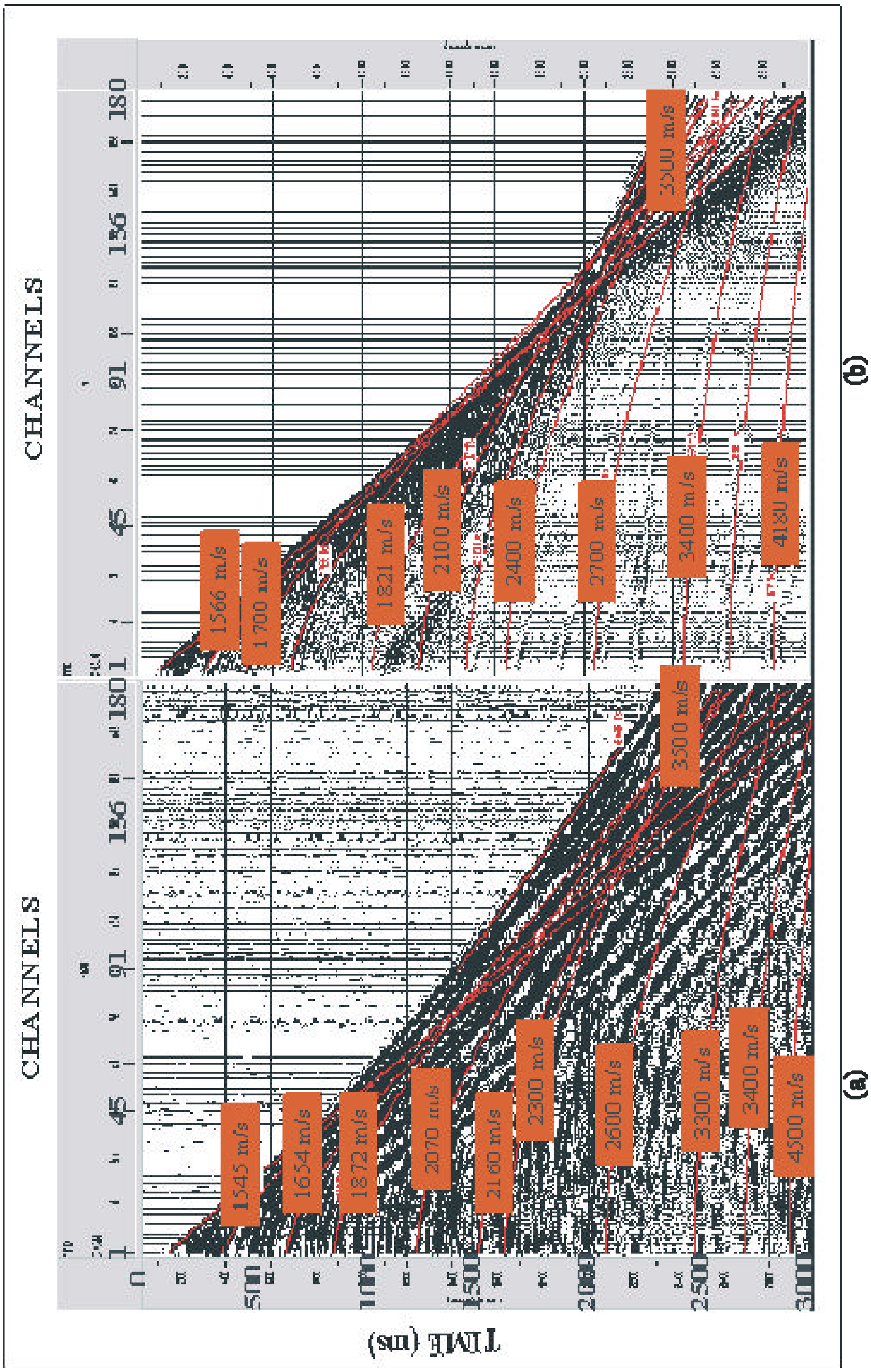

FIG. 8. Kefallinia diapir model. RMS velocities on (a) real and (b) synthetic dat

The Finite difference method properly simulates direct arrivals, reflections, diffractions, multiples and refractions. The synthetic seismograms help in recognizing seismic events present in the real data.

For the sedimentary basin, the velocity model (Fig. 5a) was deduced from the field data. In the following simulations the density was kept constant due to lack of information. An off – end array is utilized with the source at depth 7 m. The minimum offset between shot and receivers is 180 m and the receiver spacing, 25 m. The maximum depth of the model varies between 2000 m and 4000m and the recording length 2 – 3 s. The dominant frequency for the sedimentary basin model is 62.5 Hz, the grid spacing is 4.66 m, the sample rate is 1 ms. The number of time steps is 2429, the number of grid nodes in the vertical direction, 448 and in the horizontal dimension, 1311.

The synthetic data for the shot at CDP 13780 show the reflections from the major discontinuities (Fig. 6b). The RMS – velocity varies between 1500 m/s and 2300 m/s. The reflection event at 0.3 s TWT corresponds to the sea bottom. The reflections at 0.5 s TWT and 1.1 s TWT are attributed to the top and the bottom of the Upper Miocene – Lower Pliocene (Mi – Pli) sediments. The reflection event at 1.3 s TWT corresponds to the bottom of the Middle – Miocene (Mid?) sediments. These reflection events are also identified on the field data exhibiting similar reflection times and RMS velocities (Fig. 6a). This simulation helped in the identification of the major events and ensured that the velocity model of the sedimentary basin displayed in Figure 5a can be utilized for the seismic migration of the field data.

For the diapiric structure, the velocity model exhibits velocity reversals (Fig. 5b). The dominant frequency of the source wavelet is 30 Hz, the grid spacing, 9.43 m, the sample rate, 2 ms. The number of steps is 2733, the number of grid nodes in the vertical direction, 550 and in the horizontal dimension, 649.

On both the real and synthetic data (Fig. 7), the direct waves (DW) as well as reflected waves (RW) from major horizons are identified. The first arrivals on the real data for offsets greater than 930 m correspond to refracted waves. The synthetic data (Fig. 7b) additionally display a number of artificial reflections originating from artifacts of the velocity model (Fig. 5b). These artificial reflections distort major reflection events. The reflection event at 0.1 s TWT corresponds to the sea bottom. The reflection event at 1.0 s TWT present on both the field and synthetic data is attributed to the top of the Triassic evaporites. The RMS velocities for the diapir model (Fig. 8) vary between 1500 m/s and 4500 m/s.

CONCLUSIONS

The Finite difference method effectively computed synthetic seismograms for the sedimentary basin consisting of dipping layers and for the Kefallinia diapir. The Finite difference simulations verified the velocity model which resulted from seismic processing. The simulations also aided in the identification of the seismic events present on the field data.

For the sedimentary basin the reflectors at the top and the bottom of the Upper Miocene – Lower Pliocene (Mi – Pli) sediments as well as at the bottom of the Middle – Miocene (Mid?) sediments have been recognized on both the field and synthetic data. In the synthetic seismograms for Kefallinia diapir, the reflection event at 1.0 s TWT is attributed to the top of the Triassic evaporites.

Further simulations will help in the interpretation of a larger portion of the migrated section. On the other hand further simulations can be useful in refining the velocity model especially for the Kefallinia diapir. The refined velocity model deduced from the Finite difference modeling can be utilized to improve further the migrated section. Thus, seismic modeling not only recognizes seismic events present in the real data but its also useful in testing and further improving the velocity model used for the migration of the seismic section.

Table 1.

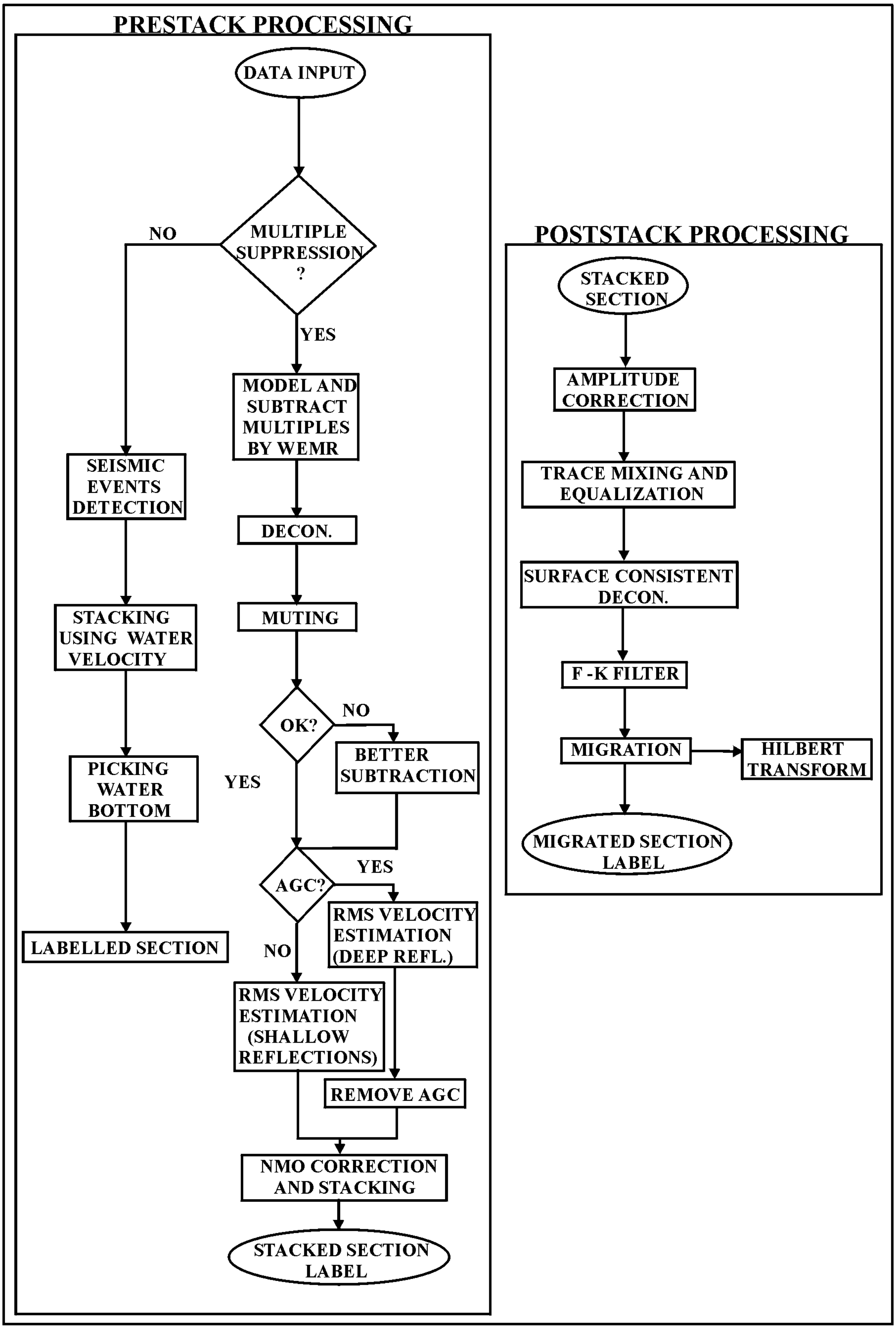
PRESTACK PROCESSING
DATA INPUT
MULTIPLE SUPPRESSION ?
NO
YES
MODEL AND SUBTRACT MULTIPLES BY WEMR
SEISMIC EVENTS DETECTION
DECON.
STACKING USING WATER VELOCITY
MUTING
OK?
NO
BETTER SUBTRACTION
YES
PICKING WATER BOTTOM
AGC?
YES
RMS VELOCITY ESTIMATION (DEEP REFL.)
NO
LABELLED SECTION
RMS VELOCITY ESTIMATION (SHALLOW REFLECTIONS)
REMOVE AGC
NMO CORRECTION AND STACKING
STACKED SECTION LABEL
POSTSTACK PROCESSING
STACKED SECTION
AMPLITUDE CORRECTION
TRACE MIXING AND EQUALIZATION
SURFACE CONSISTENT DECON.
F -K FILTER
MIGRATION
HILBERT TRANSFORM
MIGRATED SECTION LABEL

ACKNOWLEDGMENTS

The authors are deeply indebted to HELLENIC PETROLEUM Company and the University of Athens for the disposal of the data. Special thanks are due to the editors and reviewers for the suggestion of the constructive changes in this paper.

REFERENCES

Alterman, Z., and Karal, F.C., 1968, Propagation of elastic waves in layered media by finite – difference methods: Bull. Seis. Soc. Am., **58**, 367 – 398.

Biot, M.A., 1956a,Theory of propagation of elastic waves in saturated porous solid, I: Low frequency range: J. Acoust. Soc. Am., **28**, 168.

Biot, M.A., 1956b,Theory of propagation of elastic waves in a saturated porous solid, II: High - frequency range: J. Acoust. Soc. Am., **28**, 179 – 191.

Blanch, J.O., Robertson, J.O.A., and Symes, W.W., 1993, Viscoelastic finite difference modeling: 63nd SEG Annual International Meeting and Exposition, Washington D.C., Expanded Abstracts, 990 – 993.

Brew, D.S., Mayer, L.A., 1998, Modelling of Pliocene – Pleistocene abyssal mudwaves using synthetic seismograms: Marine Geology, **149**, 3 – 16.

Brokesova, J., Zahradnik, J., Paraskevopoulos, P., 2000, Ray and finite – difference modelling of CDP seismic sections for shallow lignite deposits: Journal of Applied Geophysics, **45**, 261 – 272.

Carcione, J.M., Kosloff, D., and Kosloff, R., 1988a, Wave propagation simulation in a linear viscoacoustic medium: Geophysics, **53**, 769 – 777.

Carcione, J.M., Kosloff, D., and Kosloff, R., 1988b, Wave propagation simulation in a linear viscoelastic medium: Geophys. J. Roy. Astr. Soc., **95**, 393 – 407.

Dai, N., Vafidis, A., and Kanasewich, E.R., 1995, Wave propagation in heterogeneous porous media: A velocity-stress finite difference method: Geophysics, **60**, No. 2, pp. 327-340.

De la Cruz, V., and Spanos, T.J.T., 1985, Seismic wave propagation in a porous medium: Geophysics, **50**, 1556 – 1565.

Emmerich, H., and Korn, M., 1987, Incorporation of attenuation into time domain computations of seismic wave fields: Geophysics, **52**, 1252 – 1264.

Frenje, L., Juhlin, C., 1998, Scattering of seismic waves simulated by finite difference modelling in random media: Application to the Gravberg – 1 well, Sweden: Tectonophysics, **293**, 61 – 68.

Hassanzadeh, S., 1991, Acoustic modelling in fluid saturated porous media: Geophysics, **56**, 424 – 435.

Hirn, A., Sachpazi, M., Siliqi, R., McBride, J., Marnelis, F., Cernobori, L., and STREAMERS – PROFILES group, 1996, A traverse of the Ionian islands front with coincident normal incidence/ and wide angle seismics: Tectonophysics **264**, 35 –49.

Hollinger, K., 1997, Upper - crustal velocity heterogeneities as derived from a variety of P – wave sonic logs: Geophys. J. Int., **125**, 813 – 829.

Kamberis, E., Marnelis, F., Loucoyannakis, M., Maltezou, F., Hirn, A., and STREAMERS group, 1996, Structure and deformation of the External Hellenides based on seismic data from offshore Western Greece: EAGE Special Publication **5**, 207 – 214.

Kelly, K.R., Ward, R.W., Treitel, S., and Alford R.M., 1976, Synthetic seismograms: a finite – difference approach: Geophysics, **41**, 2 – 27.

Kokinou, E., 2002, Processing and interpretation of deep seismic reflection data in Ionian sea: Ph.D. thesis, Technical University of Crete, Greece.

Kosloff, D., and Baysal, E., 1982, Forward modeling by a Fourier method: Geophysics, **47**, 1402 – 1412.

Larkin, S.P., Levander, A., Okaya, D., Goff, J.A., 1996, A deterministic and stochastic velocity model for the Salton Trough/Basin and Range transition zone and constraints on magmatism during rifting: J. Geophys. Res., **101**, 27883 – 27897.

Marfurt, K.J., 1984, Accuracy of finite difference and finite element modeling of the scalar and elastic wave equations: Geophysics, **49**, 533 – 549.

McBride, J.H., White, R.S., Henstock, T.J., and Hobbs, R.W., 1994, Complex structure along a Mesozoic sea – floor spreading ridge: BIRPS deep seismic reflection, Cape Verde abyssal plain: Geophys. J. Int., **119**, 453 – 478.

Mikhailenko, B.G., and Korneev, V.I., 1984, Calculation of synthetic seismograms for complex subsurface geometries by a combination of finite intergral Fourier transforms and finite difference techniques: J. Geophys., **54**, 195 – 206.

PROMAX 2D Reference Manual Version 6, Volume 1, 1995.

Reshef, M., Kosloff, D., Edwards, M., Hsiung, C., 1988, Three – dimensional acoustic modeling by the Fourier method: Geophysics, **53**, 1175 – 1183.

Smith, W.D., 1975, The application of finite element analysis to body wave propagation problems: Geophys. J. Roy. Astr. Soc., **42**, 747 – 768.

Tsingas, C., Vafidis, A., and Kanasewich, E.R., 1990, Elastic wave propagation in transversely isotropic media using finite differences: Geophysical Prospecting, **38**, 993 – 949.

Vafidis, A., 1988, Super computer finite difference methods for seismic wave propagation: Ph.D dissertation, University of Alberta, Edmonton.

Vafidis, A., Abramovici, F., and Kanasewich, E.R., 1992, Elastic wave propagation using fully vectorized high order finite differences: Geophysics, **57**, 218 – 232.

Vafidis, A., Dai, N., and Kanasewich, E.R., 1993, Wave propagation in viscoacoustic heterogenous media, A velocity – pressure finite – difference method: Canadian Journal of Exploration Geophysics, **29**, 402 – 410.

Zelt, C.A., 1999, Modelling strategies and model assessment for wide – angle seismic traveltime data: Geophys. J. Int., **139**, 183 – 204.

Zhu, X., and McMechan, G.A., 1991, Finite – difference modelling of the seismic response of fluid – saturated, porous, elastic media using Biot theory: Geophysics, **56**, 328–339.

.